# Efficient Manufacture, Deconstruction, and Upcycling of High-Performance Thermosets and Composites

Authors: Evan M. Lloyd[1,2,†], Julian C. Cooper[1,3†], Peyton Shieh[4,] , Douglas G. Ivanoff[1,5,] , Nil A. Parikh[1,6], Edgar B. Mejia[1,5], Keith E. L. Husted[4], Letícia C. Costa[4], Nancy R. Sottos[1,5*], Jeremiah A. Johnson[4*], Jeffrey S. Moore[1,3*]

**Affiliations:**

[1]Beckman Institute for Advanced Science and Technology, University of Illinois at Urbana-Champaign, Urbana, IL, USA.

[2]Department of Chemical and Biomolecular Engineering, University of Illinois at Urbana-Champaign, Urbana, IL, USA.

[3]Department of Chemistry, University of Illinois at Urbana-Champaign, Urbana, IL, USA.

[4]Department of Chemistry, Massachusetts Institute of Technology, Cambridge, MA, USA.

[5]Department of Materials Science and Engineering, University of Illinois at Urbana-Champaign, Urbana, IL, USA.

[6]Department of Aerospace Engineering, University of Illinois at Urbana-Champaign, Urbana, IL, USA.

*Correspondence to: n-sottos@illinois.edu, jaj2109@mit.edu, jsmoore@illinois.edu

†Denotes equal contribution.

**ABSTRACT**

Thermoset polymers and fiber-reinforced polymer composites possess the chemical, physical, and mechanical properties necessary for energy-efficient vehicles and structures, but their energy-inefficient manufacturing and the lack of end-of-life strategies render these materials unsustainable. Here, we demonstrate end-of-life deconstruction and upcycling of high-performance poly(dicyclopentadiene) (pDCPD) thermosets with a concurrent reduction in the energy demand for curing via frontal copolymerization. Triggered material deconstruction is achieved through cleavage of cyclic silyl ethers and acetals incorporated into pDCPD thermosets. Both solution-state and bulk experiments reveal that seven- and eight-membered cyclic silyl ethers and eight-membered cyclic acetals incorporate efficiently with norbornene-derived monomers, permitting deconstruction at low comonomer loadings. Frontal copolymerization of DCPD with these tailored cleavable comonomers enables energy-efficient manufacturing of sustainable, high-performance thermosets with glass transition temperatures greater than 100 °C and elastic moduli greater than 1 GPa. The polymers are fully deconstructed, yielding hydroxyl-terminated oligomers that are upcycled to polyurethane-containing thermosets with higher glass transition temperatures (ca. 158 °C) than the original polymer upon reaction with diisocyanates. This approach is extended to frontally polymerized fiber-reinforced composites, where high fiber volume fraction composites ($V_f = 65\%$) containing a cleavable comonomer are deconstructed and the reclaimed fibers are used to regenerate composites via frontal polymerization that display near identical properties compared to the original. This work demonstrates that the use of cleavable monomers, in combination with frontal manufacturing, provides a promising strategy to address sustainability challenges for high-performance materials at multiple stages of their lifecycle.

## INTRODUCTION

The demand for lightweight, high-performance materials in the transport, civil, and energy infrastructure has driven annual production of thermoset polymers in excess of 60 million tons.[1–3] Prized for high specific strength and stiffness, physical and chemical resilience, and thermal stability, thermoset-based fiber-reinforced polymer composites (FRPCs) ensure long service lives coupled with exceptional performance under demanding in-service conditions.[4] The widespread employment of covalently crosslinked polymers poses two significant environmental challenges: manufacturing energy and waste accumulation.

The production of thermoset polymers and composites for high-performance, structural applications is energy intensive. The resins are typically cured under pressure at elevated temperatures for several hours in large-scale ovens or autoclaves, consuming between $10^6$ and $10^8$ joules per kilogram of polymer produced.[5,6] The 30 m long autoclave utilized to cure the forward section of the Boeing 787 FRPC fuselage consumes more than 350 gigajoules in a single cure cycle[7]—enough energy to power 9 households in the United States for an entire year.[8] Further, methods to reclaim FRPCs are themselves energy intensive,[9] as they lack end-of-life strategies, and the chemical and thermal stability of the covalent networks formed during thermoset curing make deconstruction or recycling impractical.[2,3,10–14] For large-scale structures, even disposal is challenging. To decommission wind turbine blades, which often exceed 30 m in length and with a mass of more than 12,000 kg,[15]the FRPC structures must be sectioned into smaller components, transported to an appropriate landfill, and buried. With many of the turbine blades employed in the first-generation large-scale wind farms nearing the end of their useful lifespans, landfills are exceeding capacity (> 8,000 blades decommissioned annually).[16] To mitigate unintended negative

environmental impacts, future generations of materials must be manufactured with less energy using feedstocks that have a sustainable end-of-life plan.

Frontal polymerization (FP), a technique which harnesses the chemical energy stored within a resin to drive materials synthesis,[17] yields thermosets and FRPCs with properties nearly identical to those cured by traditional methods, while also reducing the energy required for manufacture by more than ten orders of magnitude.[18] Beyond energy savings, FP's reliance on energy stored in the monomer would dramatically reduce manufacturing costs, eliminating the need for large and expensive autoclave ovens. To date, the majority of FP resin development has centered on acrylates,[19–21] epoxies,[22–24] and strained cyclic olefins,[18,25–30] all of which lack the necessary functionality for end-of-life management. The addition of cleavable units is an attractive strategy for material deconstruction,[31,32] and recent reports of cyclic olefin monomers which install cleavable units into the polymer backbone via ring-opening metathesis polymerization (ROMP) are a promising new approach for component reclamation.[33–43] Moatsou and coworkers utilized seven-membered cyclic acetals as localized spacers in multiblock poly(norbornenes),[34] where hydrolysis of the acid-labile acetals enabled precise scission of the spacer and the release of poly(norbornene) blocks. Shieh and coworkers instead copolymerized norbornene derivatives with a cyclic eight-membered silyl ether to create cleavable linear, bottlebrush and star copolymers.[35] By incorporating this same silyl ethers into the polymer backbone of poly(dicyclopentadiene) (pDCPD),[36] Shieh and coworkers were also able to fully dissasemble pDCPD thermosets at relatively low loadings of comonomer (< 10 vol %) and use the resulting fragments to generate new pDCPD thermosets.

Inspired by recent advances in FP and cleavable ROMP polymers, we envisioned we could synthesize deconstructable thermosets and composites in an energy-efficient manner, while

revalorizing their waste products. Our strategy is summarized in **Figure 1**. Efficient manufacture of deconstructable pDCPD thermosets and composites is achieved by copolymerizing olefinic cyclic silyl ethers and cyclic acetals with DCPD using frontal ring-opening metathesis polymerization (FROMP). These silyl ethers and acetals allow for programmed deconstruction by strand cleavage—triggered by a chemical stimulus—generating oligomeric products with a high concentration of olefins and terminal hydroxyl groups that are leveraged to reclaim these deconstructed products and upcycle them to give new thermosets and composites with improved properties. Comonomer performance is evaluated by ease of comonomer synthesis, extent of copolymerization during FROMP, and ability of these comonomers to deconstruct the resulting thermoset.

## RESULTS AND DISCUSSION

Each of the monomers presented in **Figure 1** are made from commercially available precursors in either one or two easily scaled steps (See Methods Section and **Table S1**). Dichlorosilanes and aldehydes utilized in silyl ether or acetal synthesis, respectively, are available on kilogram scales from commercial sources for less than 1 USD per gram. Seven-membered cyclic silyl ethers (e.g. iPrSi-7) and cyclic acetals (e.g. iPrAc-7) are synthesized in a single, high-yield (>70 %) step from *cis*-2-butene-1,4-diol, which is commercially available for less than 0.10 USD per gram. Eight-membered cyclic silyl ethers (e.g. iPrSi-8) and cyclic acetals (e.g. iPrAc-8) are synthesized from *cis*-2-pentene-1,5-diol, obtained in one step from a commercially available lactone precursor.[44] Cyclization of this diol to form eight-membered cyclic monomers suffers from competitive oligomerization. Though the oligomers are easily removed by distillation of the desired monomer, this step requires additional energetic input and is impractical for high molecular weight species, limiting access to multifunctional monomers. Cyclization to form seven-membered cyclic olefins

is less susceptible to competitive oligomer formation. Given that the seven-membered cyclic olefins require fewer synthetic operations and are less prone to competitive oligomerization, we conclude that both iPrSi-7 and iPrAc-7 have advantages over their eight-membered counterparts.[36,40] We evaluate how effectively these monomers polymerize with norbornene-like monomers using a norbornene imide as a DCPD surrogate. Following a previously described protocol,[35] we copolymerize polyethylene glycol (PEG)-functionalized norbornene macromonomers (PEG-MM) with cleavable cyclic comonomers at various relative loadings (**Figure 2a**). Analysis of the $^{1}$H NMR spectra of the recovered copolymers containing iPrSi-8, iPrSi-7, or iPrAc-8 reveal new broad resonances in both the olefinic and allylic regions that are not present in PEG-MM homopolymer (**Figure S14-S19**). By contrast, the spectra from the copolymerization reaction with iPrAc-7 lack any of these additional signals, suggesting that iPrAc-7 does not copolymerize to an appreciable extent with PEG-MM (**Figure S20**).

Following polymerization, we proceeded to deconstruct each of the graft copolymers using a 1 M aqueous solution of HCl to hydrolyze the silyl ethers or acetals and evaluated the extent of comonomer incorporation by size exclusion chromatography (SEC). Copolymers derived from seven- and eight-membered silyl ethers, as well as eight-membered acetals readily cleave into oligomeric fragments of similar sizes, as seen by a large shift to higher elution times (**Figure 2b-d**). These results are consistent with statistical incorporation previously observed for iPrSi-8,[35] and suggest that both iPrSi-7 and iPrAc-8—while not identical to iPrSi-8—also incorporate into the polymer backbone in a near statistical fashion. However, copolymers with iPrAc-7 demonstrate minimal shift in the SEC traces after treatment with HCl, indicative of poor incorporation of the seven-membered acetal within the poly(norbornene) backbone (**Figure 2e)—**consistent with $^{1}$H NMR observations (**Figure S20**). This model system highlights the importance of tuning

comonomer structure to efficiently introduce cleavable linkages into the backbone of poly(norbornene) copolymers.

During FP, the energy density of the resin is a key factor governing the attainable front velocities. Each of the candidate monomers possess substantially less ring strain (**Table S1**) than the norbornene ring of DCPD,[45] calculated to be 26.7 kcal $mol^{-1}$. The low ring strain of the comonomers reduces the energy density of the resin, leading to decreased front velocities at increased comonomer loadings. While it is preferable to have highly strained cyclic comonomers, monomers with lower ring strain than DCPD (e.g. 1,5-cyclooctadiene,COD, with a ring strain of approximately 13.4 kcal $mol^{-1}$) have been frontally copolymerized with DCPD while maintaining rapid front velocities.[28] Even at 50 vol % COD, Dean and coworkers reported front velocities greater than 4 cm $min^{-1}$.[28] Frontal copolymerization of DCPD and cleavable cyclic olefins yields high quality materials free of voids (**Figure 3a**) for all comonomers up to the tested 25 mol % loading. Initially, the front velocity increases with increasing comonomer concentration, reaching a maximum at 2.5 mol % for iPrAc-8, 5 mol % for iPrSi-7 and iPrSi-8, and 10 mol % for iPrAc-7 (**Figure 3b**). We attribute the significantly higher front velocities for iPrAc-7 to poor incorporation during FROMP, leading iPrAc-7 to act as a passive diluent and lowering the effective activation barrier toward propagation.[46] Following this initial increase, front velocities then decay steadily due to the decrease in energy density with increased loadings of the less-strained olefins. In all cases, front velocities greater than 4 cm $min^{-1}$ are obtained, even at 25 mol % comonomer loading. We observe the relative incorporation of the energy-deficient comonomers has the greatest impact on front velocity.[18] Comonomers that incorporate in a near random fashion (iPrSi-7, iPrSi-8, and iPrAc-8), exhibit similar trends in front velocity and ring stain, yet iPrAc-8 exhibits the slowest front velocity (statistically significant differences at the 95 % confidence level). Together, these

results suggest that ring strain alone is not a prescriptive predictor of a monomers impact on front velocity, but extent of incorporation, in addition to ring-strain, must also be considered.

The addition of cleavable comonomers has a direct influence on thermomechanical performance of the resulting thermosets (**Figure 3c-e**). The incorporation of long, flexible aliphatic chains increases the confirmational degrees of freedom in the network, as well as decreases crosslink density in pDCDP ($M_c$ = 2776 ± 147 g mol $^{-1}$ for 10% iPrSi-7 vs. 2080 ± 40 g mol$^{-1}$ for neat pDCPD[29]), reducing the network's glass transition temperature ($T_g$, **Figure 3c, Figure S38-S39**). Due to the similarities in the aliphatic chain length and substituents, the comonomers that incorporate efficiently produce statistically similar trends with increasing comonomer loading. Glass transition temperature by differential scanning calorimetry (DSC) decreases from 163 ± 0.3 °C at 0 % comonomer to approximately 100 °C at 7.5 mol % comonomer. Further increasing the comonomer loading to 25 mol % yields copolymers with a $T_g$ near room temperature. Despite the decrease in $T_g$, the copolymers retain both Young's modulus and yield strength until comonomer concentration exceeds 15 mol % (**Figure 3d-e**), beyond which both the modulus and strength decrease dramatically.

To evaluate the deconstruction of the FROMP-cured thermosets, we immerse samples in solutions of either a 1.0 M tetrabutylammonium fluoride (TBAF) in THF for silyl ether-containing thermosets or 1.0 M HCl in CPME for acetal-containing thermosets (**Figure 4** and **Figures S27-S28**). although acid treatment can result in cleavage of both systems (*vide infra*). After 16 h, pDCPD lacking any cleavable comonomer remains intact, with no observable signs of deconstruction in either solution. With the introduction of cleavable comonomers, thermoset dissolution becomes apparent, and pDCPD thermosets containing at least 7.5 mol % iPrSi-7 or iPrSi-8 or 5 mol % iPrAc-8 completely disintegrate, yielding a homogeneous solution. The

loadings required to induce complete deconstruction are near identical to pDCPD thermosets made via ROMP (approximately 7 mol%),[36] suggesting FROMP and ROMP processes share substantial chemically similarities.[39] Substantially higher loadings are required to induce complete thermoset deconstruction using iPrAc-7 (ca. 15 mol %), consistent with its poor ability to copolymerize with norbornene-like copolymers. We can achieve complete deconstruction at low molar fractions (5-7.5 mol %) with minimal influence on thermoset mechanical properties using iPrAc-8, iPrSi-8, and iPrSi-7, indicating that frontal copolymerization is an energy-efficient method to generate high-performance thermosets capable of triggered deconstruction.

Deconstruction fragments are isolated as white powders from the soluble fraction of all samples that exhibit partial or complete deconstruction by dropwise precipitation into methanol. Consistent with PEG-MM polymerization, pDCPD samples fabricated with iPrSi-8, iPrSi-7, and iPrAc-8 display a strong fragment size dependence on the comonomer concentration, indicating that in FROMP, these comonomers insert in a similar manner as in ROMP conditions (**Figure S30**). We also observe minimal differences in the SEC traces of the fragments obtained from these copolymer samples at all investigated comonomer loadings (**Figure S31a-e**). In contrast, iPrAc-7 containing thermosets show weak fragment size dependence on comonomer loading, consistent with nonstatistical incorporation (**Figure S30c**), Moreover, the deconstructed fragments are significantly larger than those isolated from iPrSi-8, iPrSi-7, and iPrAc-8 containing thermosets (**Figure 4c**). These results agree with our solution state experiments and present further evidence of significant similarities between FROMP and ROMP characteristics. With thermosets that are fully deconstructed, fragments are isolated in near quantitative yield (ca. 90 % ) on gram scale and with 77 % on multigram scale. This facile and high-yield recovery of desired products is more efficient than traditional thermoset recycling efforts which are often plagued by multiple

purification steps and low yields of the desired products[11]. Furthermore, the cleaved thermoset reveals oligomers with terminal hydroxyl functionality, which we could leverage to enable new applications for the deconstructed material.

We envisioned this -OH functionality could react with a crosslinking agent to generate a new thermosetting material with distinct properties (**Figure 5a)**. To validate this concept, we utilized oligomers derived from thermosets containing iPrSi-7—the monomer exhibiting the best combination of synthetic accessibility, front velocity, and efficient deconstruction. Kendrick analysis on MALDI-TOF spectra of oligomers derived from deconstructed pDCPD containing 10 mol % iPrSi-7 confirm the presence of allyl alcohol end groups (**Figures S32-S33**). The availability of these -OH end groups is quantified using $^{1}$H NMR. Signals at 4 ppm are consistent with the methylene resonance of the allylic alcohol (**Figure 5b**). Using an internal standard, we found that these oligomers contain $5.5 \times 10^{-4}$ mmol hydroxyl units per mg of fragments (theoretical $6.5 \times 10^{-4}$ mmol/mg) To generate a new thermosetting material, we proceeded to screen the reaction of these -OH groups with 4,4'-methylenebis(phenyl isocyanate) (MDI) in the presence of various small molecules known to catalyze urethane formation (**Scheme S1**).[47] We were encouraged that in all cases, even without catalyst, we obtain new freestanding films that do not dissolve, indicating formation of a crosslinked network from these waste products (**Figure 5c** and **Figures S35-S37**).

To evaluate the effectiveness of the reclamation process, we tested the thermomechanical properties of the regenerated thermosets using dynamic mechanical analysis (DMA) and compared these properties to the original pDCPD network containing 10 mol % iPrSi-7. Thermal sweeps indicated that at room temperature all films displayed a similar elastic modulus compared to the original 10 mol % iPrSi-7 thermoset (**Figure S40**). The catalyst is critical for effective thermoset reclamation, as the film generated without catalyst fails to show a rubbery plateau. While addition

of each catalyst resulted in films that displayed a higher $T_g$ compared to the original material. The film made with diazabicyclo[2.2.2]octane (DABCO) most effectively recovers the original thermoset crosslinking density (**Figure 5d** and **Figure S40**). This new polyurethane material displays a glass transition temperature of 162 ± 4 °C, a 70 °C increase compared to the original thermoset ($T_g$ of 92 ± 3 °C), resulting in successful upcycling to generate a material with improved properties. In fact, the glass transition temperature of the polyurethane approaches that of neat pDCPD and is greater than any of the explored FROMP copolymers (**Figure 3c and S43**). We attribute the success of this upcycling to the replacement of the flexible aliphatic silyl ether in the backbone of the original material with rigid aromatic urethane linkers.

Having demonstrated the deconstruction and upcycling of thermoset materials, we proceeded to test the ability to reclaim the matrix and fiber components of FRPCs. We utilized iPrSi-7 to efficiently manufacture deconstructable FRPCs through FROMP of DCPD. Infusion of 12 plies of carbon fiber fabric with a comonomer resin (DCPD with 10 mol % iPrSi-7) and subsequent frontal polymerization through the thickness of the laminate yields void-free parts with high fiber volume fraction ($V_f$ = 64.8 %) and high stiffness (E'[20 °C] = 36.5 GPa) **Figure 6a-d**). The fabricated FRPCs display minimal reduction in stiffness or glass transition temperature ($T_g$ = 105 °C) after treatment with *aqueous* 1 M HCl solution for 24 h (**Figure 6h)**. Full deconstruction is observed only after submersion in 1 M HCl in CPME for 16 h, demonstrating that penetration of the triggering stimulus, which is facilitated by the organic solvent, is critical to deconstruction, and validating this comonomer approach for engineering applications (**Figure 6e**). These deconstruction fragments contain a similar degree of functionality ($5.1 \times 10^{-4}$ mmol -OH per mg) compared to the neat polymer thermosets, and are easily isolated from the fabric plies by simply removing the soluble fraction and rinsing the fabric with THF. Scanning electron microscopy

reveals minimal residual matrix on the fiber surface via SEM (**Figure 6f-g)**. Further, infusion of the recovered fabric with a comonomer resin (DCPD with 10 mol % iPrSi-7) and subsequent frontal polymerization produces a new FRPC that exhibits identical thermomechanical properties as the original material (**Figure 6h**). As with the non-reinforced thermosets (*vide supra*), the matrix of the FRPC is reclaimed and transformed into a polyurethane nanocomposite with a $T_g$ of 159 ± 0.6 °C using MDI and carbon nanofibers with DABCO as catalyst (**Figure S47a**). The use of cleavable comonomers combined with FROMP provide a promising strategy for fabricating regenerative FRPCs for engineering applications.

## CONCLUSIONS

Copolymerization of cleavable comonomers with DCPD via FROMP provides a rapid and energy-efficient route to high-performance thermosets capable of triggered deconstruction and upcycling. Four cleavable comonomers were evaluated according to synthesizability, performance during frontal copolymerization, and programmed deconstruction. We found that all comonomers were easily obtained in one or two synthetic steps, but seven-membered cyclic silyl ethers and acetals were synthetically more accessible compared to their 8-membered counterparts. When copolymerized with DCPD, all four comonomers supported rapidly propagating fronts and generated high quality materials with variable thermomechanical properties. Statistical incorporation of iPrSi-8, iPrSi-7, and iPrAc-8 comonomers was seen during FROMP with DCPD, yielding deconstructable thermosets with glass transition temperatures greater than 100 °C. In contrast, seven-membered cyclic acetals suffered from inefficient incorporation into the polymer network, and a relatively high concentration of acetal was needed to ensure full deconstruction. Of the four evaluated comonomers, iPrSi-7 provided the best balance of synthetic ease, performance during frontal polymerization, and facile deconstruction. Fragments of deconstruction were readily

isolated in excellent yield, and the terminal hydroxyl groups were leveraged to generate polyurethane networks upon reaction with a diisocyanate crosslinker; the resulting materials display thermomechanical properties superior to those of the parent pDCPD copolymer networks. These cleavable comonomers also enable reclamation of composite materials. Frontally polymerized FRPCs were deconstructed when manufactured using a cleavable comonomer. This deconstruction facilitated reclamation of composite fibers that could be utilized to regenerate new FRPCs displaying near identical mechanical properties to the original composite. Importantly, these composites resisted deconstruction under conditions they would potentially encounter in their in-use environment, illustrating the applicability of this approach to engineering applications. Introduction of a cleavable comonomer into thermosetting resins and composites imbues these high-performance polymeric materials with end-of-life management capabilities, and use of these deconstruction products as source for new materials synthesis presents a significant step towards a more circular life cycle for thermoset polymers.

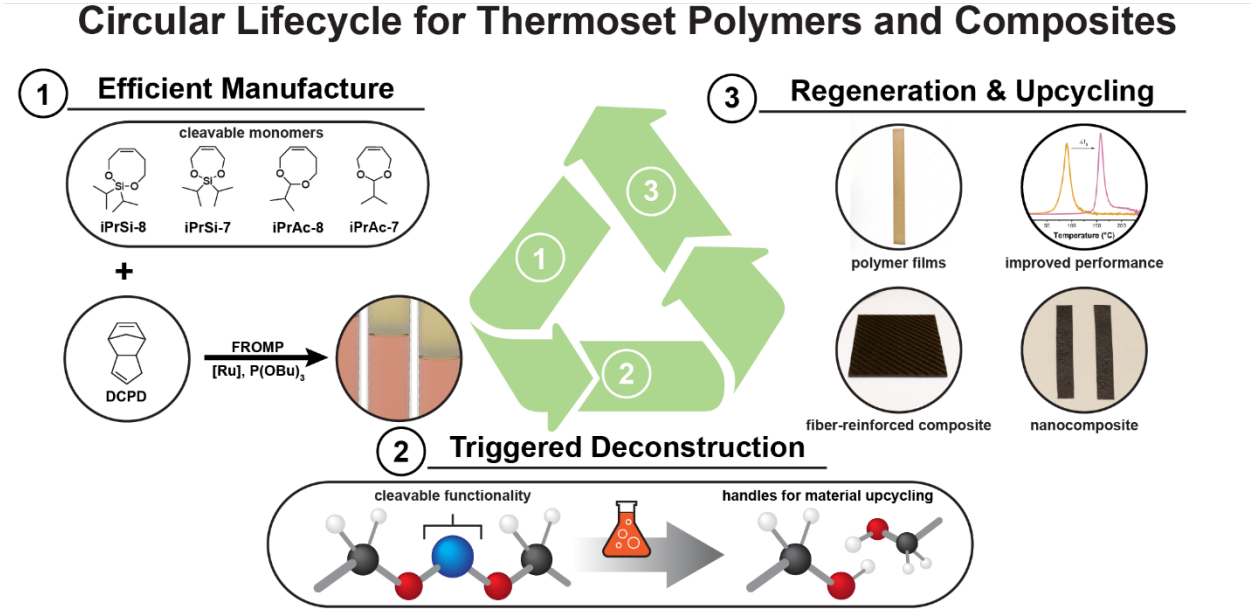


**Figure 1. Strategy for efficient manufacture, deconstruction and upcycling of thermosets and composites. 1**) Frontal copolymerization of DCPD with a cleavable monomer, mediated by a thermally activated ruthenium catalyst (e.g. 2nd generation Grubbs catalyst) and a tributyl phosphite inhibitor. **2)** Triggered deconstruction of copolymer thermoset results in products with functional handles for upcycling of these waste products **3)** Using these synthetic handles will facilitate regeneration of materials from this waste that show improved upcycled properties.

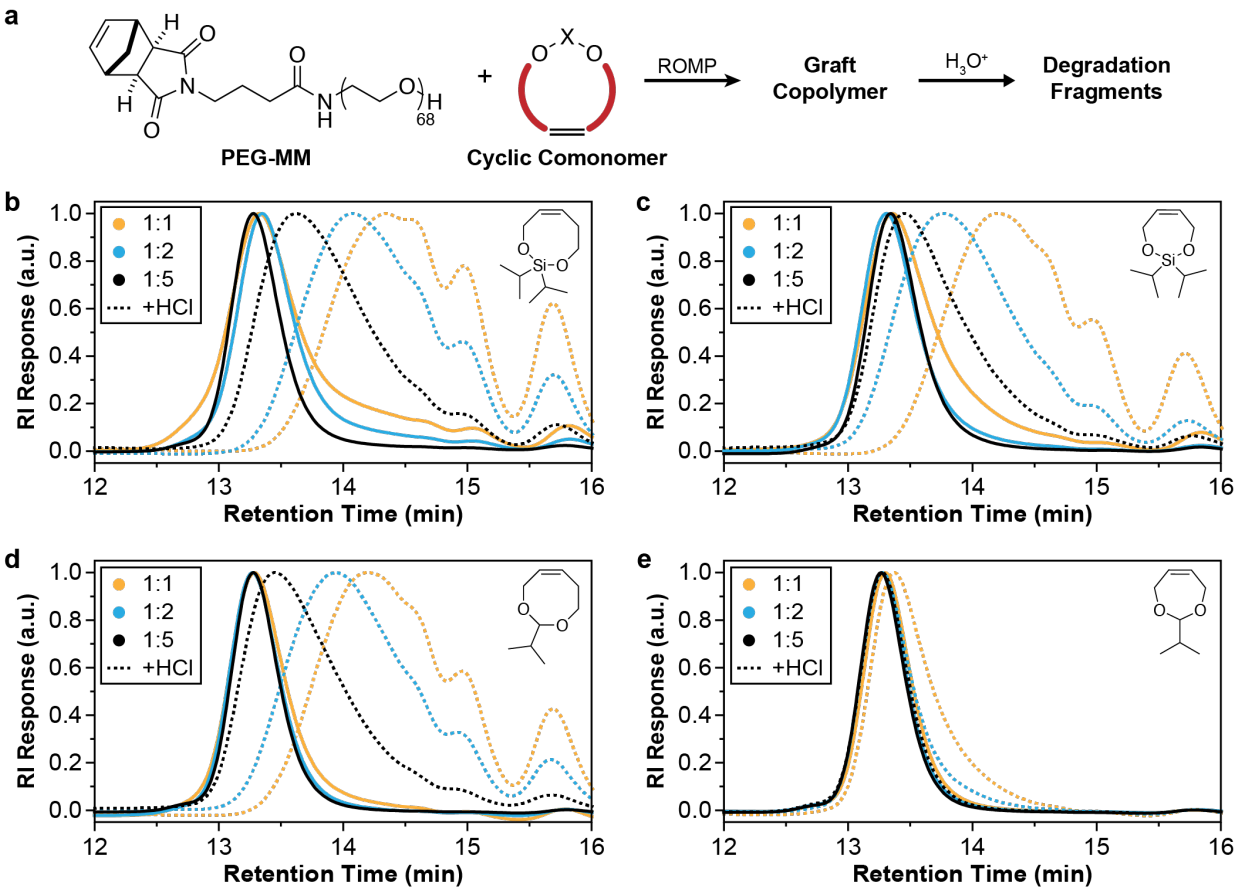


**Figure 2. Systematic evaluation of comonomer incorporation. a,** Graft copolymers were synthesized by the ring-opening metathesis copolymerization of polyethylene glycol (PEG)-norbornene macromonomers (PEG-MM) and cyclic comonomers using Grubbs' 3rd generation catalyst. A macromonomer to catalyst molar ratio of 30:1 was targeted for all experimental conditions, and cyclic comonomer to macromonomer molar ratios of 1:1, 1:2, or 1:5 were evaluated. **b-e**, Graft copolymers were analyzed by gel permeation chromatography either as synthesized (solids lines) or after hydrolytic cleavage of silyl ether or acetal linkages within the polymer backbone (dashed lines).

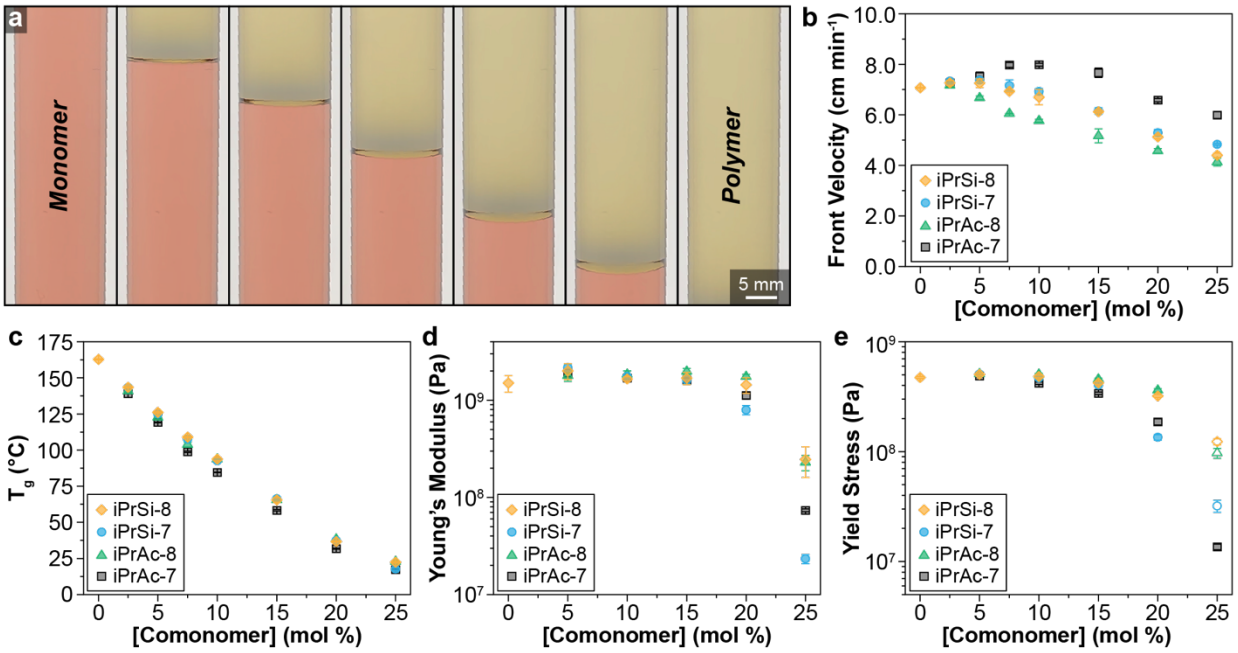


**Figure 3. Frontal ring-opening metathesis copolymerization of dicyclopentadiene and cleavable comonomers.** **a**, Optical images taken during FROMP of DCPD containing 10 mol% iPrSi-7 and 150 ppm Grubbs catalyst 2$^{nd}$ generation (GC2) inhibited with 1 molar equivalent (with respect to GC2) of tributyl phosphite (TBP). Images were taken at 5s intervals. **b**, Front velocity measured at varied loading of cleavable comonomer. All measurements were conducted at 25 °C with 150 ppm GC2 and 1 molar equivalent of TBP. Reported values represent the average and one standard deviation ($n$ = 3). **c**, Glass transition temperature ($T_g$) obtained during dynamic DSC traces (5 °C min$^{-1}$). Reported values represent the average and one standard deviation ($n$ = 3). **d**,**e** Mechanical properties of copolymers with varied loading of cleavable comonomer determined via quasi-static tensile loading. Open symbols in **e** represent the ultimate tensile strength as samples did not yield. Reported values represent the average and one standard deviation ($n$ = 5).

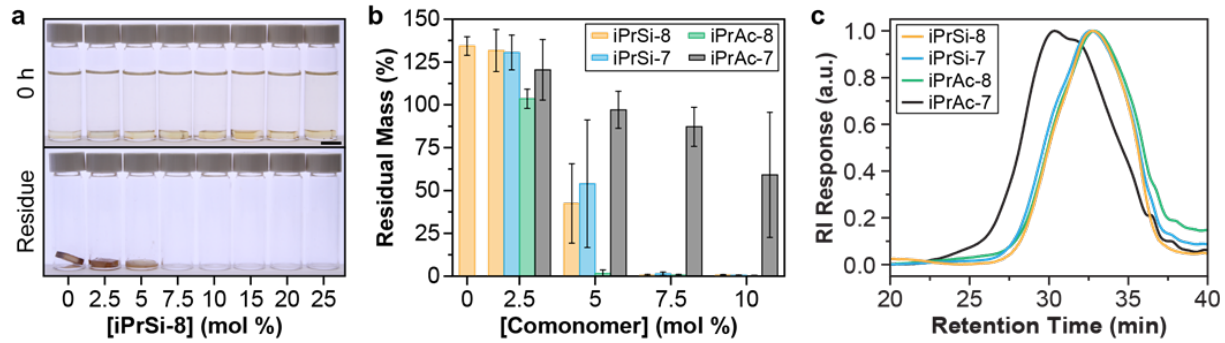


**Figure 4. Deconstruction of FROMP thermosets. a**, Optical images taken at 0 h after submerging iPrSi-8 containing thermosets in 1 M TBAF in tetrahydrofuran, and at 16 h, after removal of the soluble fraction from the residual solids. Scale bar is 1 cm. **b**, Residual mass retrieved after removing the soluble fraction at varied loading of deconstructable comonomer. Residual mass greater than 100% is a consequence of residual solvent trapped in matrix **c**, SEC traces of deconstruction fragments isolated from 15 mol % comonomer samples.

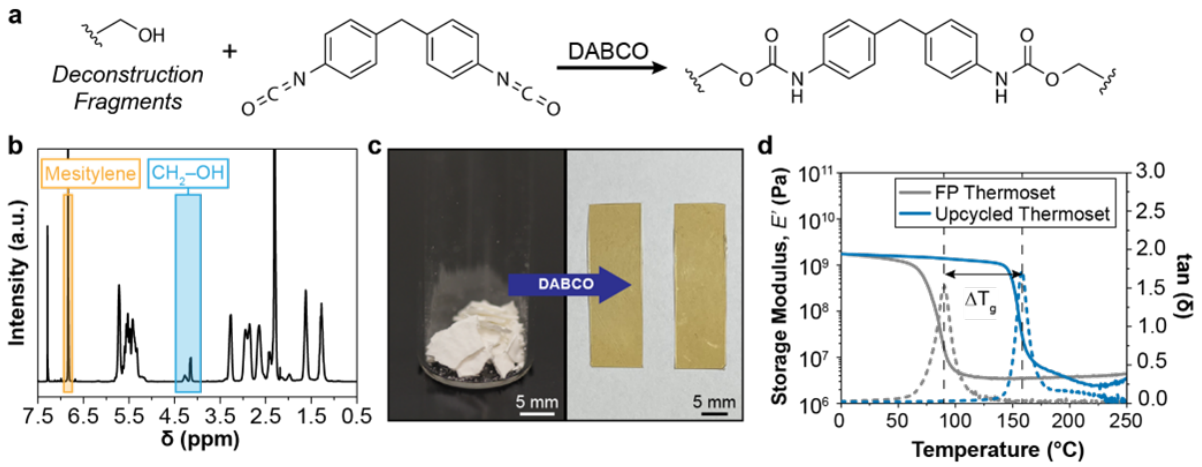


**Figure 5. Upcycling of deconstructed materials. a**, Schematic representation of the incorporation of hydroxyl-rich fragments into a polyurethane network with a diisocyanate, such as 4,4'-methylenebis(phenyl isocyanate) (MDI). **b**, $^{1}$H NMR spectrum of the fragments obtained after dismantling a thermoset containing 20 mol % iPrSi-7 with a mesitylene internal standard (500 MHz, chloroform-*d*) utilized to calculate the concentration of hydroxyl units in the fragments. **c**, Optical images of the deconstruction fragments isolated from a thermoset containing 10 mol % iPrSi-7 (left) and the free-standing films obtained after reaction with MDI. **d**, Storage modulus and tan $\delta$ traces obtained during dynamic mechanical analysis (2.0 °C min$^{-1}$) of a frontally polymerized thermoset containing 10 mol % iPrSi-7 and the upcycled polyurethane film shown in c. Upcycled film was obtained after treatment of the deconstruction fragments from a 10 mol % iPrSi-7 FP thermoset with MDI in the presence of DABCO.

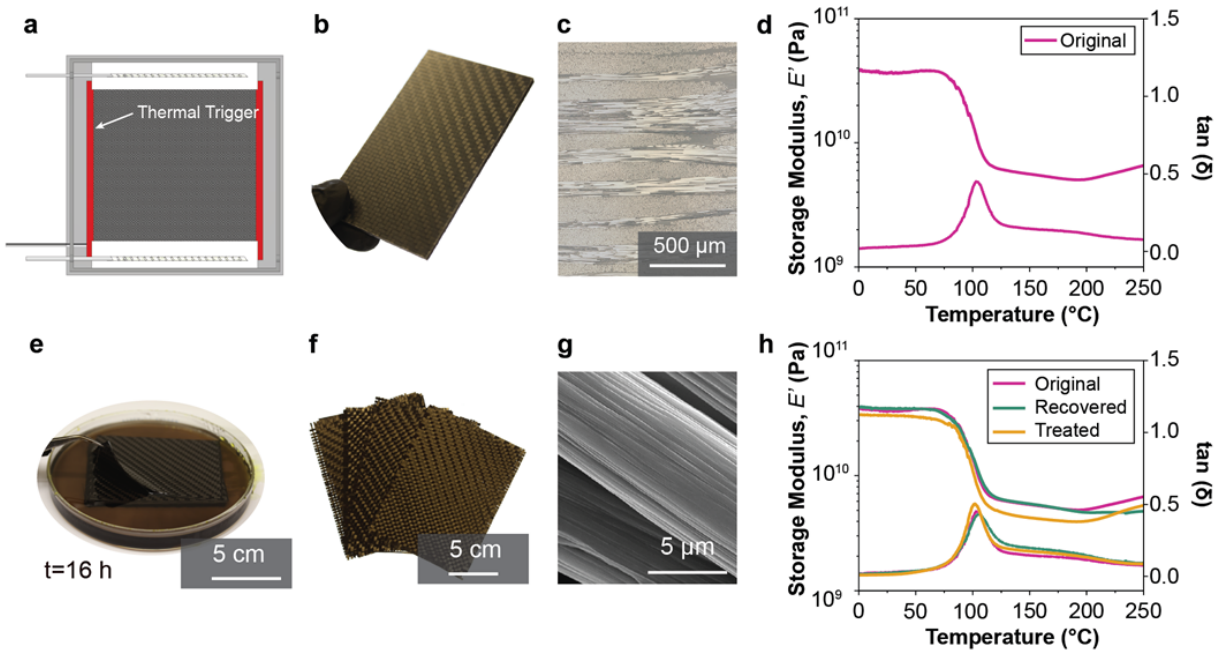


**Figure 6. Circular lifecycle of composite materials. a**, Schematic representation of fiber-reinforced polymer composites (FRPCs) fabrication through vacuum-assisted resin transfer molding (VARTM) and curing by FP through the thickness by a resistive heater (red). **b**, Optical image of the resulting FRPC containing a frontally polymerized thermoset containing 10 mol % iPrSi-7. **c**, Optical micrograph of the FRPC cross-section demonstrating a high fiber volume fraction (ca. 65%) and no void content. **d**, Representative dynamic mechanical analysis (2.0 °C $min^{-1}$) of a frontally polymerized FRPC containing 10 mol % iPrSi-7. **e**, Chemical deconstruction of the FRPC matrix using 1 M HCl in CPME and **f,** recovered fabric following deconstruction of the matrix. **g**, SEM image of the recovered carbon fiber with no evidence of matrix fragments on surface. **h** Dynamic mechanical analysis (2.0 °C $min^{-1}$) of FRPC regenerated from recovered fabric, as well as treated FRPC to simulate environmental weathering compared to the original composite.

## METHODS

*Calculation of Monomer Ring Strain*

Ring strain energies for our cleavable comonomers were calculated following an adapted literature procedure.[48] Density Functional Theory (DFT) analysis was applied to an isodesmic ring opening reaction of our cleavable comonomers with ethylene using the M06-2X functional with 6311+G(2d,p) basis set after following geometry optimization of the reactants and product. Calculations were performed on SPARTAN '18 Mechanics Program.

*Synthetic Methods*

All reagents were purchased from commercial suppliers and used without further purification. *iPrSi-8, PEG-MM, cis*-2-pentene-1,5-diol Grubbs' 3rd generation catalyst were synthesized as described previously.[35,44,49,50] $^{1}$H nuclear magnetic resonance ($^{1}$H-NMR) and $^{13}$C nuclear magnetic resonance ($^{13}$C-NMR) spectra were acquired on a Bruker Avance III 400 or a Bruker Neo 500 provided by the MIT Department of Chemistry Instrumentation Facility or on a Bruker CB500 provided by the School of Chemical Sciences NMR Laboratory at the University of Illinois at Urbana-Champaign. Chemical shifts are reported in ppm relative to signals from the NMR solvent: for $CDCl_3$, this corresponds to 7.26 for $^{1}$H and 77.2 for $^{13}$C spectra. High-resolution mass spectrometry (HRMS) measurements were obtained on a JEOL AccuTOF system at the MIT Department of Chemistry Instrumentation Facility.

*iPrSi-7*

*cis*-2-butene-1,4-diol (17.6 g, 200 mmol) was dissolved in 2 L of DCM. Next, 27.2 g (400 mmol, 2 equiv) of imidazole was added. Finally, 37.0 g of dichlorodiisopropylsilane (200 mmol, 1 equiv) in 120 mL of DCM was added dropwise over 1 h using an addition funnel. A white precipitate corresponding to the imidazolium salt formed during this time. Upon completion of addition, the reaction was filtered through a pad of silica and the silica pad washed with another 1

L of DCM. The combined filtrates were then concentrated to yield 32.6 g (81.5%) of **iPrSi-7**. The material was further purified by vacuum distillation before use in polymerization reactions. $^{1}$H NMR (400 MHz, $CDCl_3$) δ 5.66 (t, *J* = 1.9 Hz, 2H), 4.50 (d, *J* = 1.8 Hz, 4H), 1.10 (s, 12H), 1.07 (s, 2H). $^{13}$C NMR (101 MHz, $CDCl_3$) δ 129.87, 62.57, 17.33, 12.06. HRMS (DART): Predicted for $C_{10}H_{21}O_2Si$ $[M+H]^+$ 201.1311, found 201.1396.

*iPrAc-8*

*cis*-2-pentene-1,5-diol (11.7 g, 115 mmol) and trimethylorthoformate (12.2 g, 115 mmol, 1 equiv) of were added to a flask. Next, pyridinium *p*-toluenesulfonate (1.44 g 5.75 mmol, 0.05 equiv) was added and the mixture stirred for 30 minutes. The solution was then concentrated under vacuum to yield a viscous oil. Then, isobutyraldehyde (8.28 g, 115 mmol, 1 equiv) was added dropwise. A noticeable exotherm was observed over the course of the addition. The reaction was stirred for 24 h. The solution was concentrated under gentle vacuum to remove low boiling point species, distilled under vacuum, and passed through a short column of silica with 20:1 hexanes/diethyl ether to yield 8.43 g **iPrAc-8** (47.0%) as a clear oil. $^{1}$H NMR (400 MHz, $CDCl_3$) δ 5.91 (dt, J = 11.3, 7.7 Hz, 1H), 5.66 (dt, J = 11.2, 5.7 Hz, 1H), 4.31 (dd, J = 14.4, 6.5 Hz, 1H), 4.23 (d, J = 6.5 Hz, 1H), 4.08 (dd, J = 14.4, 5.0 Hz, 1H), 3.94 (ddd, J = 11.4, 6.1, 4.0 Hz, 1H), 3.42 (ddd, J = 11.9, 8.6, 3.4 Hz, 1H), 2.50 (ddt, J = 15.7, 8.0, 4.2 Hz, 1H), 2.38 (dddd, J = 14.4, 8.9, 6.3, 3.3 Hz, 1H), 1.86 (dt, J = 13.4, 6.7 Hz, 1H), 0.92 (dd, J = 6.8, 5.1 Hz, 6H). $^{13}$C NMR (101 MHz, $CDCl_3$) δ 129.43, 128.59, 107.16, 67.51, 62.35, 32.23, 28.47, 17.86, 17.34. HRMS (DART) Predicted for $C_9H_{17}O_2$ $[M+H]^+$ 157.1229, found 157.1264.

*iPrAc-7*

*cis*-2-butene-1,4-diol (15.0 g, 170 mmol), isobutyraldehyde (16.0 g, 221 mmol, 1.3 equiv), and *p*-toluenesulfonic acid monohydrate (0.97 g, 5.1 mmol, 0.03 equiv) were dissolved in 120 mL of a 2:1 mixture of dichloromethane:tetrahydrofuran in a flame-dried flask charged with a stir bar.

Sodium sulfate was added until the supernatant was clear, and the mixture was stirred overnight at room temperature. The reaction mixture was filtered and concentrated under gentle vacuum. The clear oil was purified by basic alumina column chromatography with 8:1 hexanes:ethyl acetate to yield 22.2 g **iPrAc-7** (92%) as a clear oil. $^{1}$H NMR (400 MHz, $CDCl_3$) δ 5.70 (t, *J* = 1.8 Hz, 2H), 4.39 (t, *J* = 16.4, 2.5 Hz, 2H), 4.32 (d, *J* = 6.9 Hz, 1H), 4.20 – 4.06 (d, *J* = 14.7 Hz, 2H), 1.95 – 1.81 (oct, 6.8 Hz, 1H), 0.94 (d, *J* = 6.8 Hz, 6H).$^{13}$C NMR (101 MHz, $CDCl_3$) δ 129.77, 109.13, 65.92, 31.83, 18.02.HRMS (DART) Predicted for $C_8H_{15}O_2$ $[M+H]^+$ 143.1072, found 143.1071.

*Preparation and Deconstruction of Graft Copolymers*

All procedures for graft copolymer synthesis were performed in a nitrogen-filled glovebox. 250 mg of PEG-MM was dissolved in 1000 µL dioxane. Separately, comonomers iPrSi-8, iPrSi-7, iPrAc-8, and iPrAc-7 were dissolved in dioxane to prepare 0.5 M, 0.25 M, and 0.1 M solutions. Finally, Grubbs' 3$^{rd}$ generation catalyst was dissolved in dioxane to a concentration of 0.02 M. To 0.5 dram vials, charged with a stir bar, were added 75 µL of PEG-MM solution and 11 µL of comonomer solution (or 11 µL dioxane for homopolymer synthesis). Next, 9.1 µL of G3 solution was added to target a final macromonomer to catalyst ratio of 30:1. After 30 minutes, the solutions were removed from the glovebox and quenched with a drop of ethyl vinyl ether. Aliquots of these solutions(10 µL) were dissolved in 1 mL of DMF + 0.025 M LiBr and directly characterized by analytical gel permeation chromatography (GPC) with an Agilent 1260 Infinity system with dual Agilent PL1110-6500 columns and a 0.025 M LiBr in DMF mobile phase at 60 °C. The differential refractive index of each compound was monitored using a Wyatt Optilab T-rEX detector.

A 20 µL aliquot of the copolymer solution was then mixed with 10 µL of 2 M HCl. The solution was incubated for 30 minutes. Next, an excess of sodium sulfate was added to the sample to remove residual water. Finally, the mixture was suspended in 1 mL of DMF + 0.025 M LiBr, filtered through a 0.2 µm Nylon filter, and the polymer fragments characterized by analytical GPC. The

remainder of the copolymer solution was diluted with 200 μL of chloroform and dried in a vacuum oven overnight before analysis by $^{1}$H NMR.

*Resin Preparation and Frontal Copolymerization*

To depress the freezing point of DCPD, 5 wt % ENB was blended with DCPD at 35 °C. The liquid mixture was then degassed overnight at room temperature at 15 kPa with stirring. All references to DCPD refer to the 95:5 DCPD:ENB mixture. Grubbs Catalyst 2$^{nd}$ Generation (GC2, 3.50 mg, 1 equiv) was carefully weighed out in a scintillation vial. In a separate scintillation vial, tributyl phosphite (TBP, 1.1 μL, 1 equiv) was added to DCPD (3.63 g, 6.67 × 10$^{3}$ equiv). The monomer/inhibitor solution was transferred to the vial containing GC2, and the mixture was sonicated for 10 min to ensure complete dissolution of the catalyst. The resins were filtered with a 0.45 μm polytetrafluoroethylene syringe filter to remove any debris. Comonomer resins were prepared analogously, and the total monomer concentration was maintained at 6,667 molar equivalents with respect to GC2.

Dogbone molds with gauge dimensions of 25.4 mm × 3.75 mm × 4.00 mm were fabricated with RTV-630 silicone rubber compound. A glass slide (75.0 mm × 25.0 mm × 1.00 mm was clamped to the open surface of the mold, and the molds were equilibrated at 25.0 °C in a MicroClimate environmental chamber from Cincinnati Sub-Zero. The freshly prepared resin was transferred into the mold with a syringe and equilibrated at 25.0 °C for 5 min prior to initiation. Frontal polymerization was initiated by placing the tip of a 40 W soldering iron (Weller, WLC100) at setting 5 onto the glass surface. The soldering iron tip was removed immediately after fronts were successfully initiated (ca. 2-3 s). The polymerization front position was tracked optically by video within the gauge region of the mold, and the front velocity was calculated as the slope of the best-fit line of the position over time data. All measurements were conducted at 25.0 °C within the

environmental chamber. Samples were cooled to room temperature prior to removing them from the molds.

*Solid State Deconstruction and Upcycling*

Material containing the cleavable comonomer was charged into a round bottom flask containing a stir bar and submerged in a large excess of 1 M solution of TBAF in THF (11.6 mL per g materials for 10 mol % iPrSi-7 and) and stirred for 16 h overnight, ensuring that the material was completely submerged while stirring. The next day, the resulting cloudy brown solution was precipitated dropwise into cold methanol (~40 mL per g material), and the deconstructed material then isolated by filtration. To further purify the deconstructed material, the pale orange precipitate was redissolved in minimal THF and reprecipitated in cold methanol (~40 mL per g material) to give a white solid (76.7 % recovery for 10 mol % iPrSi-7).

Size exclusion chromatography (SEC) of the pDCPD deconstruction fragments was performed on an Agilent 1260 Infinity system equipped with an isocratic pump; degasser; autosampler; a series of 4 Waters HR Styragel columns (7.8 × 300 mm, HR1, HR3, HR4, and HR5); and a triple detection system that includes an Agilent 1200 series G1362A Infinity Refractive Index Detector (RID), a Wyatt Viscostar II viscometer detector, and a Wyatt MiniDAWN Treos 3-angle light-scattering detector in THF at 25 °C and a flow rate of 1 mL $min^{-1}$. The concentration of reactive -OH functionality in the deconstructed material was quantified by $^{1}H$ NMR ($CDCl_3$, 500 MHz) using mesitylene as an added internal standard and integrating the region corresponding to the $CH_2$-OH. Quantifications were performed in duplicate.

Upcycling was performed on material derived from 10 mol% iPrSi-7 ($5.5 \times 10^{-4}$ mmol -OH per mg). A 20 mL scintillation vial was charged with deconstructed material (400 mg) with DCM (1 mL per 100 mg deconstructed material) and sonicated to dissolve. Then, catalyst (either DABCO, DPP, or DBTDL, 0.2 equiv. relative to –OH content) was added with 5 mg of magnesium

sulfate ($MgSO_4$ anhydrous) and sonicated. The mixture was filtered, removing all solid magnesium sulfate, and 2 mL of DCM were used to rinse and transfer any remaining content. Finally, methylene diphenyl isocyanate (MDI, 0.5 equiv. relative to –OH content) was added to the mixture and was sonicated for another 3 min. The resulting homogeneous solution was cast into a PTFE-lined petri dish and placed in a DCM saturated environment with a small container full of desiccant for 16 h to allow slow solvent evaporation. The resulting film was dried in vacuo, starting at room temperature 4 hours followed by 75°C for 16 h at 0.2 Torr.

Fabrication of the nanocomposite from the deconstructed FRPC followed a similar procedure to films. The deconstructed matrix ($5.1 \times 10^{-4}$ mmol -OH per mg) was dissolved in DCM (100 mg/mL) until obtaining a homogeneous mixture. The mixture was then charged with DABCO (20 mol % relative to available -OH groups) and magnesium sulfate ($MgSO_4$ anhydrous), followed by filtration. The mixture was charged with graphitized carbon nanofibers (iron-free, composed of conical platelets, D × L 100 nm × 20-200 μm, 15 wt. % with respect to deconstructed matrix) and sonicated for 15 minutes to disperse. Finally, methylene diphenyl isocyanate (MDI, 0.5 equiv. relative to -OH content) was added to the mixture and was sonicated for another 3 min. The resulting mixture was poured into a PTFE-lined petri dish and placed in the same environment as the regular films. The drying procedure was the same as the one described previously.

*Materials Characterization*

Tensile testing of pDCPD and comonomer dogbone specimens (previously listed dimensions) were performed at room temperature using an Instron 5984 universal testing system equipped with a laser extensometer and 5 kN load cell. An extension rate of 5 mm $min^{-1}$ was applied until sample failure. Elastic modulus was calculated by the slope of a best-fit line over the 0.1 % to 0.4 % strain region of the stress-strain curve. Yield strength was calculated at the point where the slope of the

stress-strain curve equaled zero. The thermomechanical properties of FP thermosets and upcycled films were evaluated with dynamic mechanical analysis (DMA). DMA tests on films (10.0 mm width and ~ 200 μm thickness) were performed on a TA Instruments RSA G2 with supplied tensile grips under a nitrogen environment. The gauge length was maintained at 10.0 mm, and a dynamic loading was applied at 1 Hz and 0.1 % strain amplitude. The temperature was increased linearly at 2.0 °C·min$^{-1}$ from -20 to 250 °C.

## ASSOCIATED CONTENT

### Supplementary Information:

The Supplementary Information is available free of charge on the Nature Publications website.

Additional experimental details and characterization data (PDF).

## AUTHOR INFORMATION


### Corresponding Authors:

*Email: n-sottos@illinois.edu jaj2109@mit.edu, jsmoore@illinois.edu


### Author Contributions:

†E.M.L. and J.C.C. contributed equally. J.S.M., N.R.S., and J.A.J. directed this research. J.S.M., N.R.S., J.A.J., E.M.L., J.C.C. and P.S. conceived the idea. E.M.L., J.C.C., P.S., D.G.I., N.A.P., E.B.M., K.E.L.H, and L.C.C. performed the experiments and analyzed the experimental data. All authors participated in writing this manuscript.

### Notes:

Authors declare no competing interests. All data is available in the main text or the Supporting Information.

## ACKNOWLEDGEMENTS


The authors acknowledge Prof. Scott White, an excellent mentor and world-leading scientist as the inspiration of this work. The authors thank the Beckman Institute for Advanced Science and

Technology, the School of Chemical Sciences NMR Laboratory, and the MIT Department of Chemistry Instrumentation Facility for the facilities and support to effectively conduct this research. The authors gratefully acknowledge the support of NSF through both the Center of Molecularly Optimized Networks (21-16298) and Grant Opportunities for Academic Liaison with Industry (19-33932), and the Air Force Office of Scientific Research through the Center of Excellence in Self-Healing, Regeneration, and Structural Remodeling (Award FA9550-16-1-0017),and NSF Leap High. E.M.L., J.C.C., and N.A.P. thank the Arnold and Mabel Beckman Foundation for financial support.

## REFERENCES

1. Chu, S. & Majumdar, A. Opportunities and challenges for a sustainable energy future. *Nature* **488**, 294–303 (2012).
2. Ma, S. & Webster, D. C. Degradable thermosets based on labile bonds or linkages: a review. *Prog Polym Sci* **76**, 65–110 (2018).
3. Post, W., Susa, A., Blaauw, R., Molenveld, K. & Knoop, R. J. I. A Review on the potential and limitations of recyclable thermosets for structural applications. *Polym Rev* **60**, 1–30 (2019).
4. Brøndsted, P., Lilholt, H. & Lystrup, A. Composite materials for wind power turbine blades. *Annu Rev Mater Res* **35**, 505–538 (2005).
5. Boluk, M. Y., Aktik, M. & Bilgen, E. Energy requirements and cost in polymer curing processes. *Energy* **15**, 811–820 (1990).
6. Abliz, D. *et al.* Curing methods for advanced polymer composites - a review. *Polymers & Polymer Composites* **21**, 341–348 (2013).
7. Timmis, A. J. *et al.* Environmental impact assessment of aviation emission reduction through the implementation of composite materials. *Int J Life Cycle Assess* **20**, 233–243 (2014).
8. 2015 Residential Energy Consumption Survey Data. https://www.eia.gov/consumption/residential/data/2015/ (2015).
9. Rani, M., Choudhary, P., Krishnan, V. & Zafar, S. A review on recycling and reuse methods for carbon fiber/glass fiber composites waste from wind turbine blades. *Compos Part B Eng* **215**, 108768 (2021).
10. Pickering, S. J. Recycling technologies for thermoset composite materials–current status. *Compos Part Appl Sci Manuf* **37**, 1206–1215 (2006).
11. Schneiderman, D. K. & Hillmyer, M. A. 50th anniversary perspective: there is a great future in sustainable polymers. *Macromolecules* **50**, 3733 3749 (2017).
12. Garcia, J. M. & Robertson, M. L. The future of plastics recycling. *Science* **358**, 870–872 (2017).
13. Di, J., Reck, B. K., Miatto, A. & Graedel, T. E. United States plastics: large flows, short lifetimes, and negligible recycling. *Resour Conservation Recycl* **167**, 105440 (2021).

14. Navarro, C. A. *et al.* A structural chemistry look at composites recycling. *Mater Horizons* **7**, 2479– 2486 (2020).
15. Red, C. Wind turbine blades: big and getting bigger. https://www.compositesworld.com/articles/wind-turbine-blades-big-and-getting-bigger (2008).
16. Martin, C. Wind turbine blades can't be recycled, so they're piling up in landfills. https://www.bloomberg.com/news/features/2020-02-05/wind-turbine-blades-can-t-be-recycled-so-they-re-piling-up-in-landfills (2020).
17. Pojman, J. A. *Frontal Polymerization*. vol. 4 (Elsevier B.V., 2012).
18. Robertson, I. D. *et al.* Rapid energy-efficient manufacturing of polymers and composites via frontal polymerization. *Nature* **557**, 223–227 (2018).
19. Pojman, J. A. Traveling fronts of methacrylic acid polymerization. *J Am Chem Soc* **113**, 6284–6286 (1991).
20. Nason, C., Roper, T., Hoyle, C. & Pojman, J. A. UV-induced frontal polymerization of multifunctional (meth)acrylates. *Macromolecules* **38**, 5506–5512 (2005).
21. Holt, T., Fazende, K., Jee, E., Wu, Q. & Pojman, J. A. Cure-on-demand wood adhesive based on the frontal polymerization of acrylates. *J Appl Polym Sci* **133**, (2016).
22. White, S. R. & Kim, C. A simultaneous lay-up and in situ cure process for thick composites. *J Reinf Plast Comp* **12**, 520–535 (1993).
23. Chekanov, Y., Arrington, D., Brust, G. & Pojman, J. A. Frontal curing of epoxy resins: comparison of mechanical and thermal properties to batch-cured materials. *J Appl Polym Sci* **66**, 1209–1216 (1997).
24. Lecompère, M., Allonas, X., Maréchal, D. & Criqui, A. Versatility of pyrylium salt/vinyl ether initiating system for epoxide dual-cure polymerization: kick-starting effect of the coinitiator. *Macromol Rapid Comm* **38**, 1600660 (2017).
25. Mariani, A., Fiori, S., Chekanov, Y. & Pojman, J. A. Frontal ring-opening metathesis polymerization of dicyclopentadiene. *Macromolecules* **34**, 6539–6541 (2001).
26. Robertson, I. D., Pruitt, E. L. & Moore, J. S. Frontal ring-opening metathesis polymerization of exo-dicyclopentadiene for low catalyst loadings. *ACS Macro Lett* **5**, 593–596 (2016).
27. Robertson, I. D. *et al.* Alkyl phosphite inhibitors for frontal ring-opening metathesis polymerization greatly increase pot life. *ACS Macro Lett* **6**, 609–612 (2017).
28. Dean, L. M., Wu, Q., Alshangiti, O., Moore, J. S. & Sottos, N. R. Rapid synthesis of elastomers and thermosets with tunable thermomechanical properties. *ACS Macro Lett* **9**, 819–824 (2020).
29. Ivanoff, D. G., Sung, J., Butikofer, S. M., Moore, J. S. & Sottos, N. R. Cross-linking agents for enhanced performance of thermosets prepared via frontal ring-opening metathesis polymerization. *Macromolecules* **53**, 8360–8366 (2020).
30. Lloyd, E. M. *et al.* Spontaneous patterning during frontal polymerization. *ACS Central Sci* **7**, 603–612 (2021).
31. Ebdon, J. R. Synthesis of new telechelic oligomers and macro-monomers by "constructive degradation." *Macromol Symp* **84**, 45–54 (1994).
32. Kiel, G. R. *et al.* Cleavable comonomers for chemically recyclable polystyrene: a general approach to vinyl polymer circularity. *J Am Chem Soc* **144**, 12979–12988 (2022).
33. Chang, C.-C. & Emrick, T. Functional polyolefins containing disulfide and phosphoester groups: synthesis and orthogonal degradation. *Macromolecules* **47**, 1344–1350 (2014).

34. Moatsou, D., Nagarkar, A., Kilbinger, A. F. M. & O'Reilly, R. K. Degradable precision polynorbornenes via ring-opening metathesis polymerization. *J Polym Sci Part Polym Chem* **54**, 1236–1242 (2015).
35. Shieh, P., Nguyen, H. V.-T. & Johnson, J. A. Tailored silyl ether monomers enable backbone-degradable polynorbornene-based linear, bottlebrush and star copolymers through ROMP. *Nat Chem* **11**, 1124–1132 (2019).
36. Shieh, P. *et al.* Cleavable comonomers enable degradable, recyclable thermoset plastics. *Nature* **583**, 542–547 (2020).
37. Feist, J. D. & Xia, Y. Enol ethers are effective monomers for ring-opening metathesis polymerization: synthesis of degradable and depolymerizable poly(2,3-dihydrofuran). *J Am Chem Soc* **142**, 1186–1189 (2020).
38. Liang, Y., Sun, H., Cao, W., Thompson, M. P. & Gianneschi, N. C. Degradable polyphosphoramidate via ring-opening metathesis polymerization. *ACS Macro Lett* **9**, 1417–1422 (2020).
39. Hsu, T.-G. *et al.* A polymer with "locked" degradability: superior backbone stability and accessible degradability enabled by mechanophore installation. *J Am Chem Soc* **142**, 2100–2104 (2020).
40. Shieh, P., Hill, M. R., Zhang, W., Kristufek, S. L. & Johnson, J. A. Clip chemistry: diverse (bio)(macro)molecular and material function through breaking covalent bonds. *Chem Rev* **121**, 7059–7121 (2021).
41. Husted, K. E. L., Shieh, P., Lundberg, D. J., Kristufek, S. L. & Johnson, J. A. Molecularly designed additives for chemically deconstructable thermosets without compromised thermomechanical properties. *ACS Macro Lett* **10**, 805–810 (2021).
42. Huang, B. *et al.* Backbone-Photodegradable polymers by incorporating acylsilane monomers via ring-opening metathesis polymerization. *J Am Chem Soc* **143**, 17920–17925 (2021).
43. Feist, J. D., Lee, D. C. & Xia, Y. A versatile approach for the synthesis of degradable polymers via controlled ring-opening metathesis copolymerization. *Nat Chem* **14**, 53–58 (2022).
44. Tomooka, K., Miyasaka, S., Motomura, S. & Igawa, K. Planar chiral dialkoxysilane: introduction of inherent chirality and high reactivity in conventional achiral alkene. *Chem - European J* **20**, 7598–7602 (2014).
45. Njoroge, I., Kempler, P. A., Deng, X., Arnold, S. T. & Jennings, G. K. Surface-initiated ring-opening metathesis polymerization of dicyclopentadiene from the vapor phase. *Langmuir* **33**, 13903–13912 (2017).
46. Masere, J., Stewart, F., Meehan, T. & Pojman, J. A. Period-doubling behavior in frontal polymerization of multifunctional acrylates. *Chaos Interdiscip J Nonlinear Sci* **9**, 315–322 (1999).
47. Sardon, H. *et al.* Synthesis of polyurethanes using organocatalysis: a perspective. *Macromolecules* **48**, 3153–3165 (2015).
48. Tuba, R., Al-Hashimi, M., Bazzi, H. S. & Grubbs, R. H. One-pot synthesis of poly(vinyl alcohol) (pva) copolymers via ruthenium catalyzed equilibrium ring-opening metathesis polymerization of hydroxyl functionalized cyclopentene. *Macromolecules* **47**, 8190–8195 (2014).
49. Love, J. A., Morgan, J. P., Trnka, T. M. & Grubbs, R. H. A practical and highly active ruthenium-based catalyst that effects the cross metathesis of acrylonitrile. *Angewandte Chemie Int Ed* **41**, 4035–4037 (2002).

50. Liu, J. *et al.* “Brush-first” method for the parallel synthesis of photocleavable, nitroxide-labeled poly(ethylene glycol) star polymers. *J Am Chem Soc* **134**, 16337–16344 (2012).